University of Tehran Press

Online ISSN: 2345-475X

DESERT

Home page: https://jdesert.ut.ac.ir/

Assessment of Fire Risk in Fars Province Based on Random Forest Model and Remote Sensing Data

Mohammad Reza Kargar[1*], Morteza Taripanah[2], Elmira Asadi-Fard[3], Seyed Kazem Alavipanah[4]

[1] Department of Forest Science, Faculty of Natural Resources and Marine Sciences, University of Tarbiat Modares, Noor, Iran. Email: mohammadreza_kargar@modares.ac.ir
[2] Department of Forestry and Forest Economics, Faculty of Natural Resources, University of Tehran, Karaj, Iran.
[3] Department of Environmental Sciences, Faculty of Natural Resources and Marine Sciences, Tarbiat Modares University, Noor, Iran.
[4] Department of Remote Sensing and GIS, Faculty of Geography, University of Tehran, Tehran, Iran.

Article Info.

Article type:
Research Article

Article history:
Received: 21 Jan. 2026
Received in revised from: 15 Jun. 2026
Accepted: 18 Jun. 2026
Published online: 27 Jun. 2026

Keywords:
Fire,
Predictions,
Random Forest,
Sentinel 2,
Evaluation.

ABSTRACT

Fire risk prediction is critical for mitigating the devastating environmental and socio-economic impacts of wildfires. In this study, one of the machine learning methods was utilized for Fars Province, Iran, based on remote sensing data and geospatial (ground measurement) data. Noticeably, twelve important variables were considered, including physiographic variables (elevation, slope, aspect), climatic variables (max temperature, precipitation, humidity), human activity factors (distance to roads, settlements, rivers, agricultural lands), and vegetation variables (land use, vegetation type). The model was developed specifically for the summer/peak fire season and it was trained and validated on dataset of 1,089 historical fire incident points from 2019 to 2022, with sentinel-2 imagery used for visual validation of burned areas. The Random Forest model illustrated high ability and performance according to assessment section results; the Kappa coefficient was about 83 percent and important factors in this process included land use, vegetation type, and absolute maximum summer temperature. The findings indicated that fire occurrence is most strongly associated with the fourth class of elevation (1834–2289 m), the second class of slope, and, for distance maps, the first class of road map, settlement, river, and agricultural lands. This highlights the significant role of human ignition sources and specific environmental conditions. The fire risk map effectively categorizes the province into areas of differing vulnerability, offering a comprehensive, adaptable, and practical resource for land managers. This facilitates the formulation of tailored preventative strategies, optimal resource allocation, and a proactive methodology for wildfire management in diverse and vulnerable ecosystems.

Cite this article: Kargar, M.R., Taripanah, M., Asadi-Fard, E., Alavipanah, S.K. (2026). Assessment of Fire Risk in Fars Province Based on Random Forest Model and Remote Sensing Data. DESERT, 31 (1), DOI: 10.22059/jdesert.2026.108250

DOI: 10.22059/jdesert.2026.108250

Publisher: University of Tehran Press

1. Introduction

Fires have been a major environmental issue (Yang *et al*., 2021), causing damage to property and human lives, as well as to the environment by altering ecosystem functioning, structure, and services. They are also regarded as a major source of greenhouse gas emissions (Kim and Sarkar, 2017; Michael *et al*., 2021). Additionally, fires are seen as a problem due to short-term and long-term health risks, economic losses, and the emission of CO_2 into the environment (Chowdhury and Hassan, 2015). The smoke, particle matter (PM), and carbon monoxide (CO) produced by fires can cause fatal diseases such as lung cancer, heart disease, and respiratory issues, especially in coastal areas and main roads which experienced the most pollution (Forsberg *et al*., 2012; Yu *et al*., 2017; Yousefi Kebriya *et al*., 2025). Conversely, children and adults experience psychological depression (Yu *et al.*, 2017). As a result, it is critical to be able to foresee fires and take preventative actions to lessen their disastrous effects (Yang *et al*., 2021). But in general, it is difficult to accurately predict the time and place of fire occurrence (Polat *et al*., 2020).

As a result, current fire monitoring and forecast systems in natural resource areas that rely on meteorological and remote sensing data mostly use modeling techniques and manually created features to make predictions (Chowdhury and Hassan, 2015; Yu *et al*., 2017; Yang *et al*., 2021). In this regard, fire risk maps are crucial and can be created using high-quality continuous spatial and temporal data from satellites (Helman, 2018; Michael *et al*., 2021). Making decisions for wildfire prevention and fire expansion measures is aided by these maps, sometimes referred to as fire hazard maps, which map the likelihood of a fire occurring (Szpakowski and Jensen, 2019; Michael *et al*., 2021).

Nonetheless, a popular method for study in this area is the application of a logistic regression (LR) model, which is constrained by the constraints of normalcy and linear correlations but may forecast the incidence of fires in response to various geographic variables (Guo *et al*., 2016). LR is frequently used for binary outcomes, such as whether fire is present or not. In contrast, wildfire science and management make extensive use of machine learning (ML) techniques, a type of artificial intelligence (Milanović *et al*., 2020).

Among the different machine learning techniques, Random Forest (RF) is a machine learning algorithm that can dynamically assess the intricate relationship between factors and automatically choose significant variables. RF has demonstrated superior predictive capacity over multiple linear regression and logistic regression in the investigation of forest fire causing elements (Ma *et al*., 2020). Biophysical and social variables can have complicated and nonlinear interactions. However, RF (a non-parametric methodology) is regarded to be a more flexible method to evaluate complex interactions among variables since it can automatically choose the key variables, regardless of how many variables are initially utilized, and does not experience the problem of over-fitting (Oliveira *et al*. 2012; Guo *et al*., 2016).

Beyond these broad benefits, RF has demonstrated efficacy in processing remote sensing data for investigations pertaining to fires. In particular, the limitations of simple linear regression models in complex heterogeneous landscapes that generally generate low inter-class discrimination and high intra-class variation, can be overcome through supervised classification of remote sensing data using machine learning techniques such as RF (Collins *et al*., 2018; Gibson *et al*, 2020).

This model classifier outperforms the other machine learning techniques (Hultquist *et al*., 2014) and provides extremely accurate classification, which is especially useful for mapping fire severity (e.g. Meddens *et al*., 2016; Meng *et al*., 2017; Collins *et al*., 2018; Parks *et al*., 2019; Collins *et al*, 2020). RF classifiers with multiple spectral indices produce better fire severity maps (LIKE Normalized Burn Ratio) than traditional methods with a single spectral inde (Collins *et al*., 2018; Gibson *et al*., 2020). Consequently, RF-based severity mapping is computationally efficient and can be automated), offering an opportunity to improve the quality and accuracy of fire severity datasets (e.g., Monitoring Trends in Burn Severity) both in the past and into the future (Parks *et al*., 2019; Collins *et al*.,2020). The quality and features of the training data are another important factor that needs to be considered and are crucial for the effective use of this model. Up until an asymptote is reached, increasing the quantity of training data should increase model accuracy (Belgiu and Drăguţ, 2016; Gibson *et al*.,2020).

This research used RF to estimate fire danger in Fars Province using a wide range of ground-based and remote sensing factors, taking into account these capabilities and data requirements. In this study, we utilized RF (Random Forest) model for predicting fire risk/occurrence at regional scale (Fars province) based on crucial variables such as Elevation, Slope, Geographical Directions, Vegetation Variables, Human Factors and Climatic Variables. Because 86% of historical fire events occurred in summer, the model was developed specifically to characterize fire risk during the summer/peak fire-danger season in Fars Province. This kind of modeling and the result, map of fire risk can be considered as guidelines for the planning and implementation of fire prevention measures, particularly the design of forest management strategies adjusted to the conditions of different ecosystems.

2. Materials and methods

2.1. Case Study

The study area is Fars province in the arid and semi-arid region, and it is located in the Southwest of Iran ($27°0\acute{3}$ and $31°4\acute{2}$ N and $50°3\acute{0}$ and $55°3\acute{6}$ E). The area of this province is about 123946 Km^2 with arid and semi-arid climate. This province is bordered to the north by Isfahan, Kohgiluyeh and Boyer-Ahmad, to the east by Yazd and Kerman, to the west by Bushehr, and to the south by Hormozgan. Fars Province has diverse ecosystems, and as a result, the lands of the province feature various land uses, including forests, rangeland, and salt flats (Ahani *et al*., 2012; Azadi and Karimi-Jashni, 2016; khabazi *et al*., 2025). Figure 1 represents the study area.

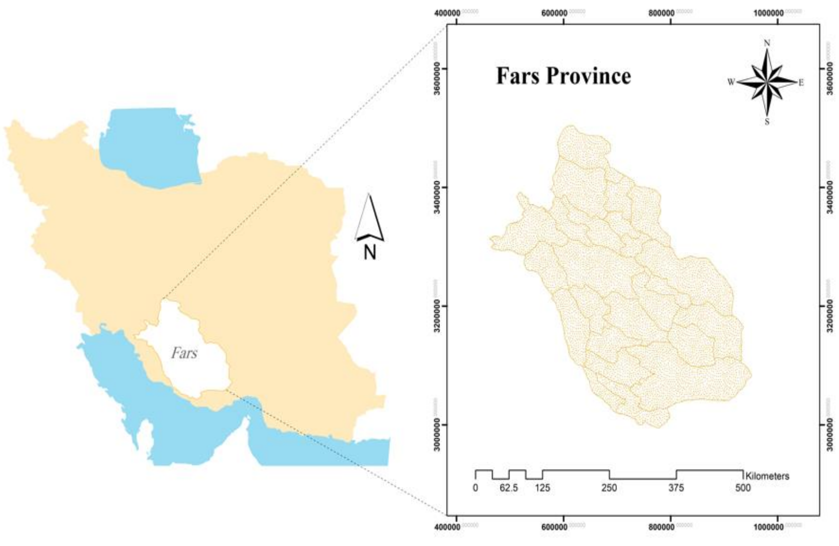

Figure 1. Location of Study area (Fars province)

2.2. Remotely Sensed Data and Field Measurement

In this study we used sentinel-2 data (Composite of bands 4, 8, and 12) from March 2019 until March 2022 (https://browser.dataspace.copernicus.eu) for assessment part (fire or no fire, accurate or inaccurate location) and these were for visual display only. This band combination (12, 8, 4) is supported by literature. Silva *et al*. (2021) explicitly recommended the SWIR2M(12)–NIR(8)–BLUE (2) composition as the most suitable for visual interpretation of fire scars and burned areas, while Bar *et al*. (2020) employed the SWIR–NIR–Blue band combination to demonstrate its effectiveness for forest fire patch identification using machine learning classifiers (Bar *et al*., 2020; Silva *et al*., 2021).

ALOS PALSAR data were also used for Fars province (https://search.asf.alaska.edu/). ALOS PALSAR data were used solely to generate the 12.5-m digital elevation model (DEM) for deriving physiographic variables (elevation, slope, aspect).

Then, the history of recorded fire incidents in the relevant departments (The General Directorate of Environmental Protection of Fars Province and General Department of Natural Resources and Watershed Management of Fars Province) and meteorological stations data for this study area for this period were collected. As illustrated in Figure 2, there are 230 climatology stations (green) and 23 synoptic stations (red). It should be mentioned that we added the seasonal breakdown of the fire inventory (86% summer vs. 14% other seasons) to make the temporal structure of the training data transparent.

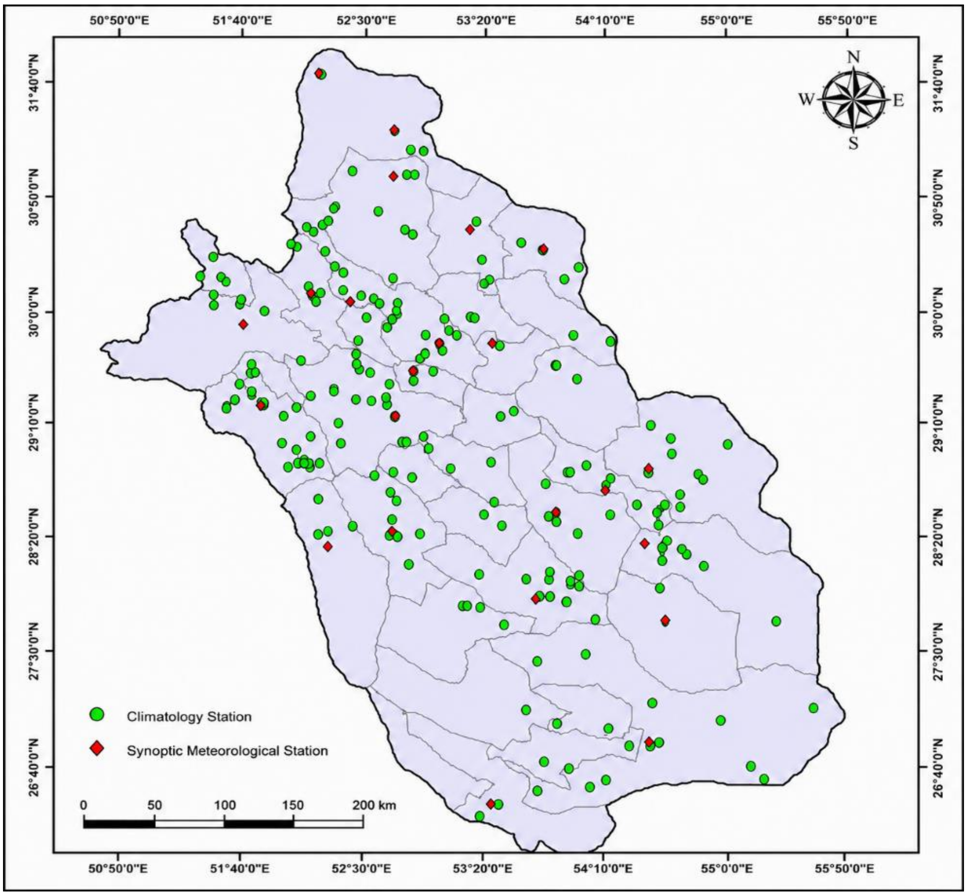

Figure 2: Distribution of meteorological stations in Fars Province; green points represent climatology stations (230 stations) and red points represent synoptic stations (23 stations)

2.3. Methods

2.3.1. Determining and extracting indicators affecting fire

In this study, 12 variables (in four categories such as physiographic, climatic, vegetation, and human factors) were utilized for preparing the fire risk prediction map, including three physiographic variables, three climatic variables, five human factors, and one cover variable. For the physiographic variables map, the 12.5-meter digital elevation model of the Alos Palsar satellite was used. The physiographic maps used in this study include elevation, slope, and geographic direction maps. The climate variables used in this study are absolute maximum summer temperature, average summer rainfall, and average relative summer humidity. Average summer relative humidity (%) was calculated as the mean of daily relative humidity during the summer months for the years 2019–2022. Relative humidity data were obtained from meteorological stations, and the continuous surface map was generated using the Inverse Distance Weighting (IDW) interpolation method, following the same procedure applied to temperature and precipitation.

Satellite Sentinel-2 and Google Earth images were also utilized to make the human impact variables map. In this part, maps of distance from the villages, access routes, rivers, agricultural lands and land use maps were prepared. In the arid and semi-arid context of Fars province, distance to rivers is considered a human-related factor because riverbanks attract recreational human activities (e.g., camping, cooking) that serve as primary ignition sources.

The cover map used in this study includes vegetation type (landcover) map. This map (land cover) and land use (Human Factors category) were produced by classification Sentinel-2 imagery based on the Random Forest algorithm (RF), following standard preprocessing steps including atmospheric and geometric correction. Training samples were collected from high-resolution Google Earth imagery and field knowledge. The classification achieved an overall accuracy of 85%, as validated by independent reference points (more details in Table 1).

Table 1. Effective Indicators included in four categories such as physiographic, climatic, vegetation, and human factors variables on fire Incidents

	Category	**Effective Indicator**
Effective Indicators of Fire Incidents	Physiographic Variables	Elevation Slope Geographical Directions (Aspect)
	Climatic Variables	Absolute Maximum Summer Temperature Average Summer Precipitation Average Summer Relative Humidity
	Vegetation Variables	Vegetation Type
	Human Factors	Distance from Road Distance from Settlements Distance from Rivers Distance from Agricultural Lands Land Use

2.3.2. Modeling procedure

Machine learning algorithms have demonstrated enormous potential for mapping environmental data across diverse contexts (Collins *et al*., 2020). Because a rule-based method ensures that the inaccuracy of a single classification is outweighed by the ensemble of several classifications, these algorithms can significantly increase accuracy. The iterative nature of Random Forest (RF-Machine learning algorithm), an ensemble learning technique, ensures a convergence-based approach to classification (Gibson *et al*., 2020). Strong predictive accuracy and remarkable flexibility in assessing complicated variable interactions are achieved by this method. Its non-parametric structure, which makes use of majority voting, which naturally resists over-fitting, and its inherent capacity to automatically discover significant variables from a sizable starting pool are the sources of its resilience (Guo *et al*., 2016; Collins *et al*., 2020). Consequently, RF classifiers provide extremely precise categorization, making them especially helpful for mapping fire severity (Collins *et al*., 2020).

After preparation layer/maps (based on effective indicators on fire incidents) according to Figure 3, geometric processing was done. In this part, it included an examination of the pixel size and the extent of each layer effective in the modeling process. If these two factors are not consistent across different layers and the layers do not align properly, the modeling process will not be carried out correctly. For modeling by the random forest algorithm, the R programming language and caret were used. First, using the commands of these packages, the importance of each layer and, in a way, their impact on the modeling process were determined. Of the sampling data, 75% was randomly selected as training data and 25% as testing data for modeling.

2.3.3. Assessment

For the assessment of model, the AUC, TSS, Kappa coefficient and overall accuracy metrics were applied. The Kappa formula presented in Eq (1). It should be mentioned that the fires that occurred in Fars province were also investigated by sentinel-2 images to evaluate the performance of the model in period time of study. The description of the Eq. (1) is given in Table 2.

$$\widehat{K} = \frac{N \sum_{i=1}^{K} x_{ii} - \sum_{i=1}^{k} (x_{i+} \times x_{+j})}{N^2 - \sum_{i=1}^{k} (x_{i+} \times x_{+j})} \qquad \text{Eq (1)}$$

Table 2. Detail of the variables Eq. (1)

Variables	Description
$\mathbf{x_{ii}}$	The elements on the main diagonal of the error matrix
$\mathbf{x_{i+}}$	The sum of row i in the error matrix
$\mathbf{x_{+j}}$	The sum of column j in the error matrix
N	The total number of samples or pixels

2.3.4. Sensitivity Analysis

Sensitivity analysis in data mining and statistical modeling typically pertains to assessing the significance of drivers inside the respective models, reflecting the relative importance of the variables employed in an artificial neural network (Asadi-Fard *et al*., 2024).

3. Results

After reviewing the history of recorded fire incidents in the relevant departments and revealing and detecting the burned areas from satellite images, 1089 fire points were prepared for the years 2019,2020, 2021 and 2022. More information is presented in Table 3, separately.

Table 3. Frequency of Fire Incident at study area

Years	Number of Fire Incident Locations
March 2019- March 2020	107
March 2020- March 2021	729
March 2021- March 2022	253

To assess the historical record of fire incidents, remote sensing data from Sentinel-2 were employed. A composite image was generated by combining bands 4 (Red), 8 (Near-Infrared), and 12 (Short-Wave Infrared). This specific band combination effectively enhanced the spectral signature of burn scars, allowing the locations of past fire events to be clearly identified in the resulting imagery, as presented in Figure 3.

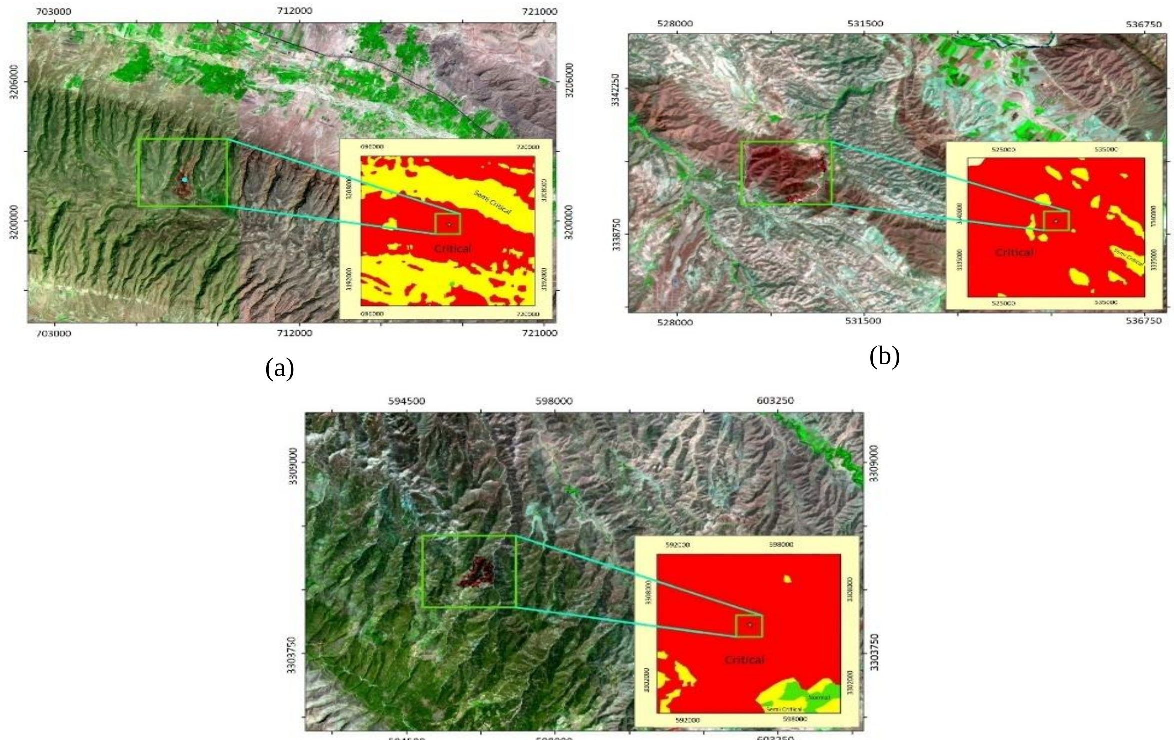

(a) (b)

(c)

Figure 3. Fire/burned areas in three parts that were labeled as critical points in three pictures such as (a), (b), and (c) in Fars province detected based on sentinel-2 data (Composite of bands 4, 8, and 12) from March 2019 until March 2022.

3.1. Physiographic Variables

-Elevation

The elevation map was made (According to Figure 4). Then, fire hotspots were located on it (elevation map). According to Table 3, the highest fire incidents are in class four elevation with 29.84% (1834-2289 meters). The lowest one with 13.13% was related to the class one elevation.

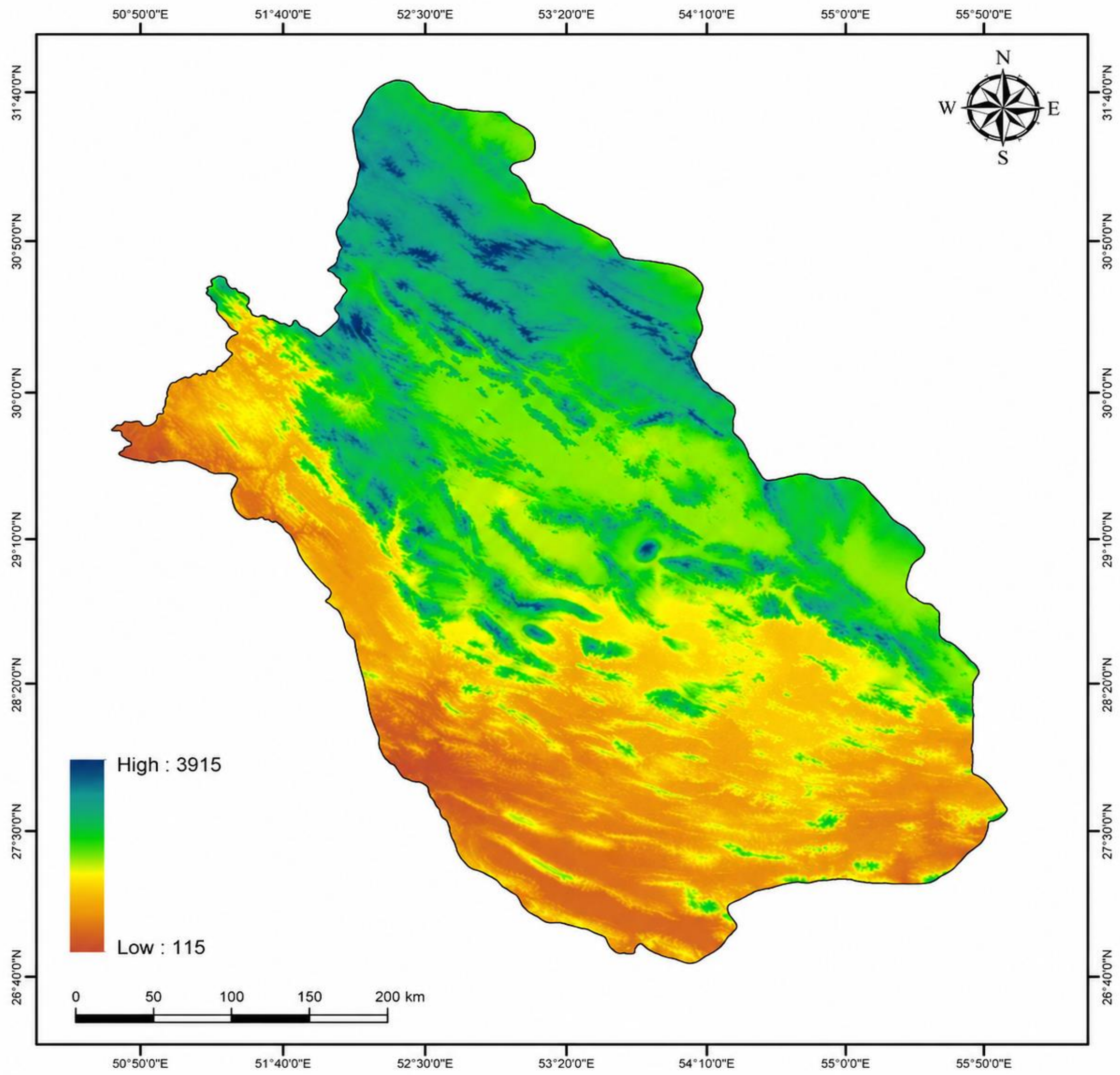

Figure 4. The elevation (m) map in Fars Province, the highest rate of elevation in Fars province is 3915 (m), and the minimum one is 115 (m).

Table 4. Geographical distribution of fire incidents in elevations classes

Elevation classification (m)	Fire Incidents No.	Fire Incidents (%)
115-846	143	13.13
846-1339	210	19.28
1339-1834	210	19.28
1834-2289	325	29.84
2289-3915	201	18.45
Total	1089	100.00

-Slope

The slope map was prepared based on DEM[1] (Figure 5) and then the fire areas were placed on it. According to Table 5, the highest rate of fire areas with 29.56% occurred in the slope class of 4.79-11.44 degrees. Also, the lowest rate of fire is related to the areas with the highest slope (29.54-67.88 degrees).

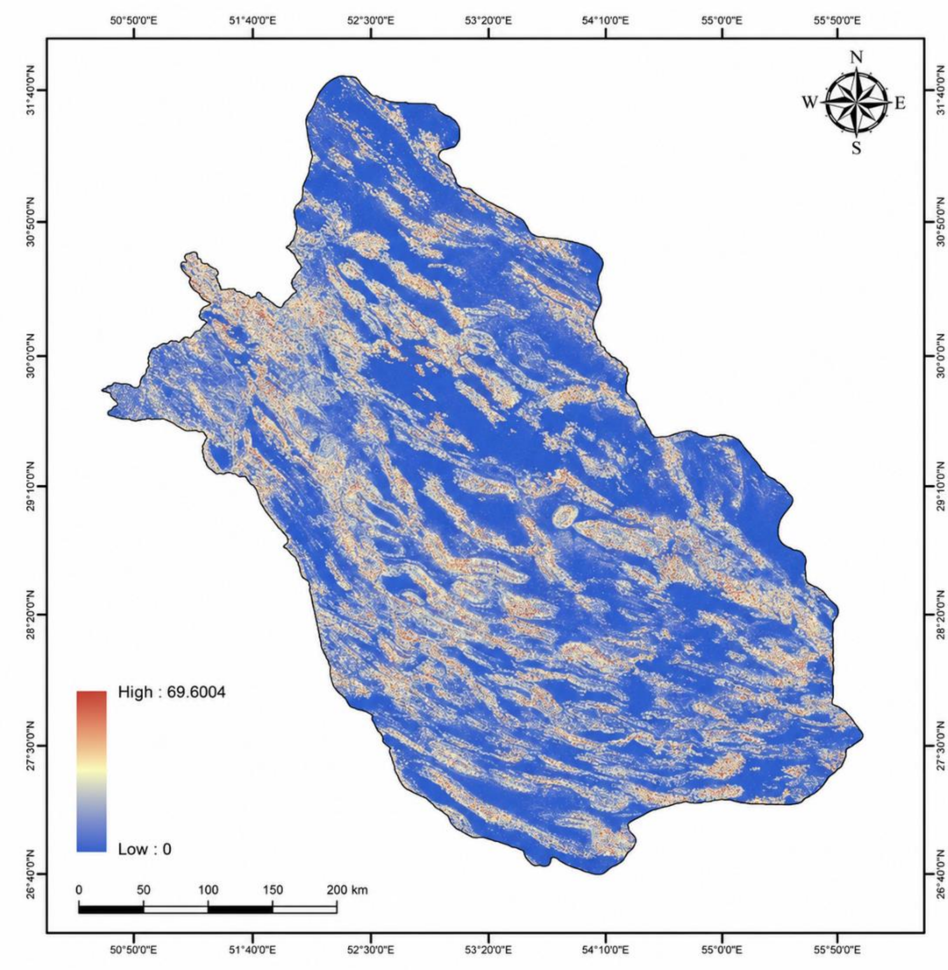

Figure 5. The slope map of Fars province the highest degree of slope in Fars province is 69.6004 (degree), and the minimum one is 0 (degree).

Table 5. Geographical distribution of fire incidents in slope classes

Slope classification (degree)	Fire Incidents No.	Fire Incidents (%)
0-4.79	315	28.92
4.79-11.44	322	29.56
11.44-19.43	274	25.16
19.43-29.54	148	13.59
29.54-69.6004	30	2.75
Total	1089	100.00

[1] Digital elevation model

- Geographical Directions (Aspect)

The Geographical directions map was prepared (Figure 6). After locating the fire areas (incidents) on the map, and based on the values in Table 6, it was determined that the highest fire rate with 27.91% occurred in the southern directions. The lowest fire rate with 0.45% occurred in the flat areas.

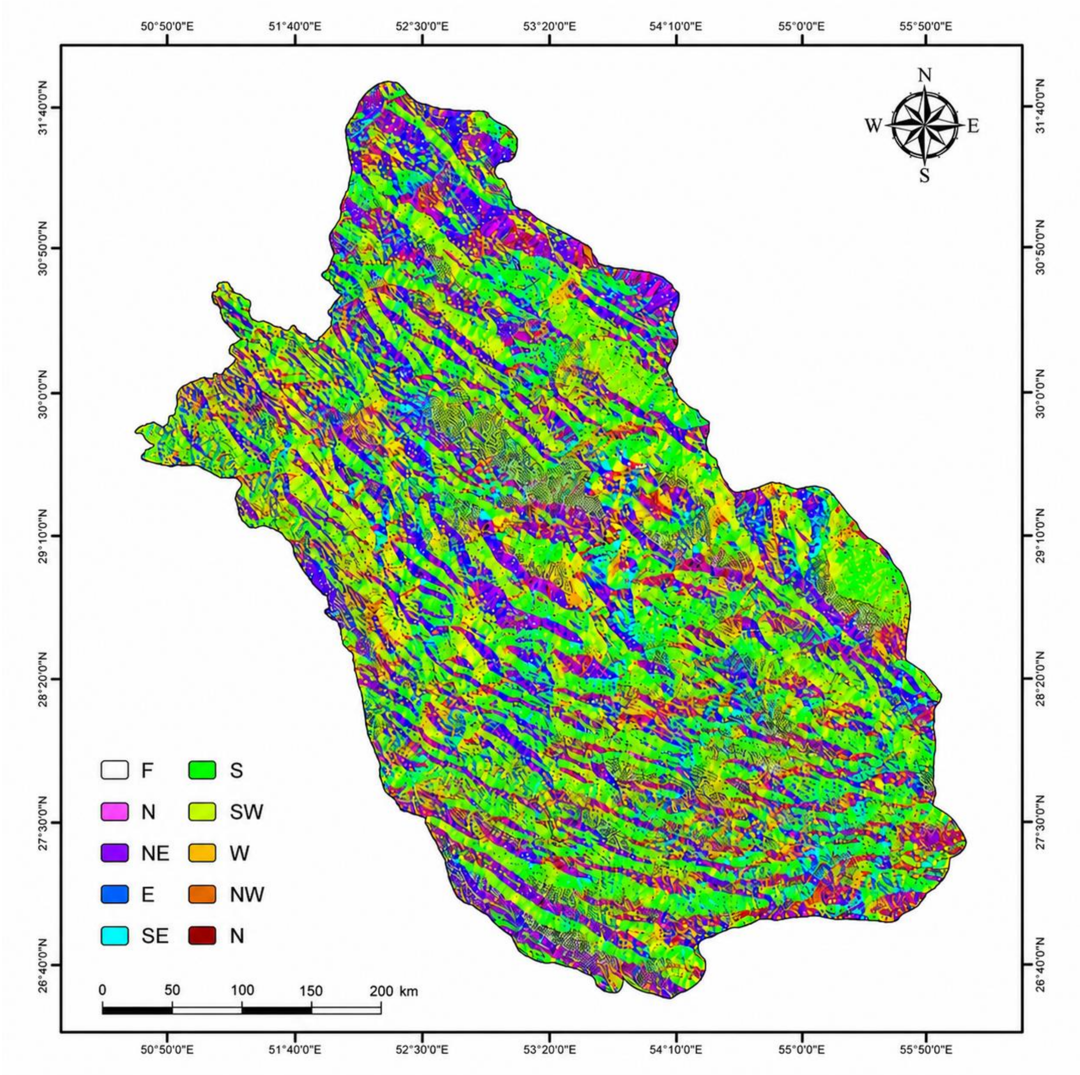

Figure 6. Geographical Directions map of Fars Province

Table 6. Geographical distribution of fire incidents in geographical directions

Geographical Directions	Fire Incidents No.	Fire Incidents (%)
Flat	5	0.45
North	263	24.15
East	287	26.35
South	304	27.91
West	230	21.12
Total	1089	100.00

3.2. Vegetation Variable:

-Vegetation Type (cover)

This map illustrates a Vegetation Type/cover classification of Fars province based on Sentinel-2 satellite data. It focuses specifically on the density and type of forest cover (e.g., Dense, Sparse, Semi-dense, Planted), rangeland density, scrubland and shrubland, and reedbed areas. The most common vegetation cover was assigned to the Sparse Rangeland (low-density) and the lowest one is allocated to the Dense Rangeland (according to Figure 7).

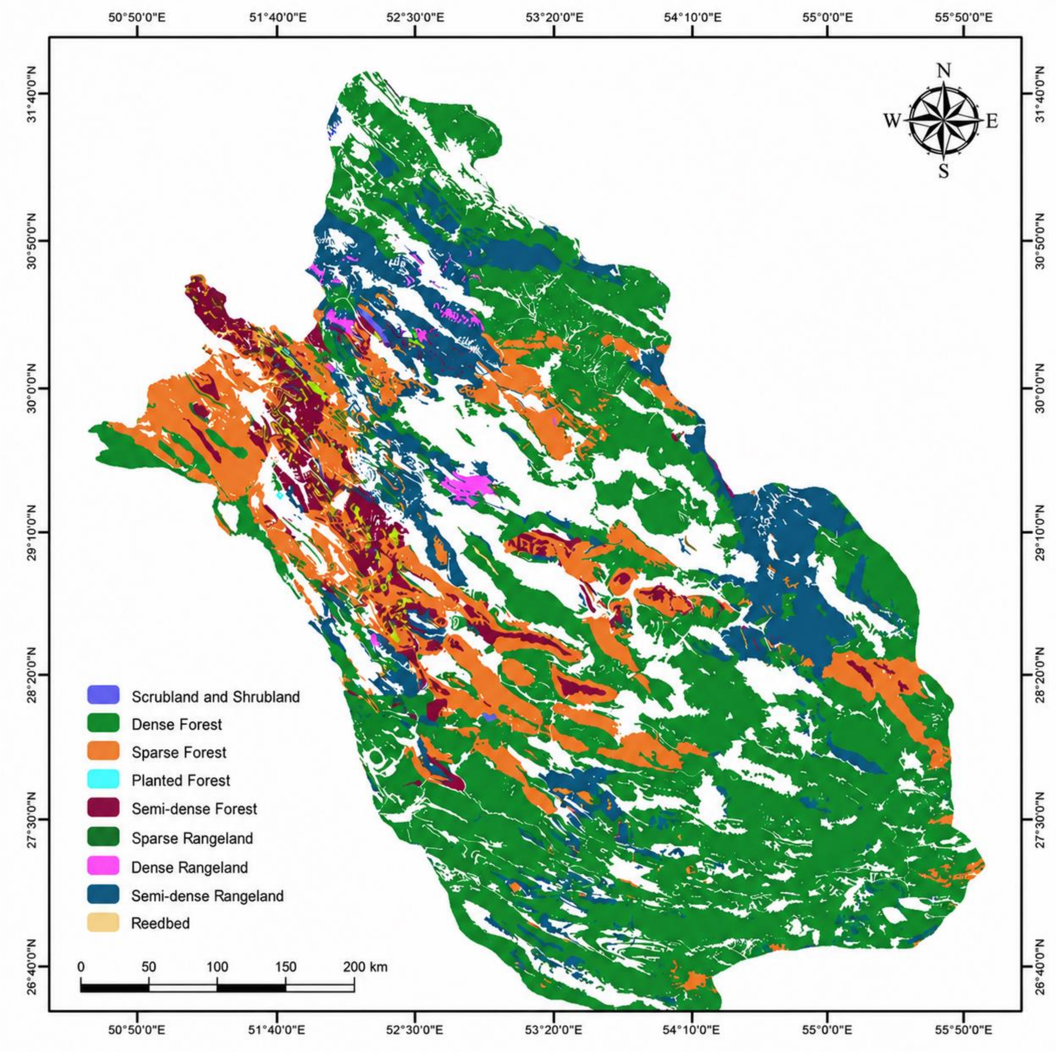

Figure 7. Vegetation Cover (Type) map Fars province (based on classification and Sentinel-2 data including various types of forest, rangeland scrubland and shrubland, and reedbed areas)

3.3. Human Factors

For this variable, a map of distance from the road, settlements, rivers and agricultural lands and land use map were prepared. The highest fire incidents and rate of them were about the first class of distance maps. In the distance maps for roads, settlements, rivers, and agricultural lands, the smaller the distance from the desired target, the more fires occurred in those areas (According to Figures 8,9,10,11 and 12; Tables 7,8,9 and 10).

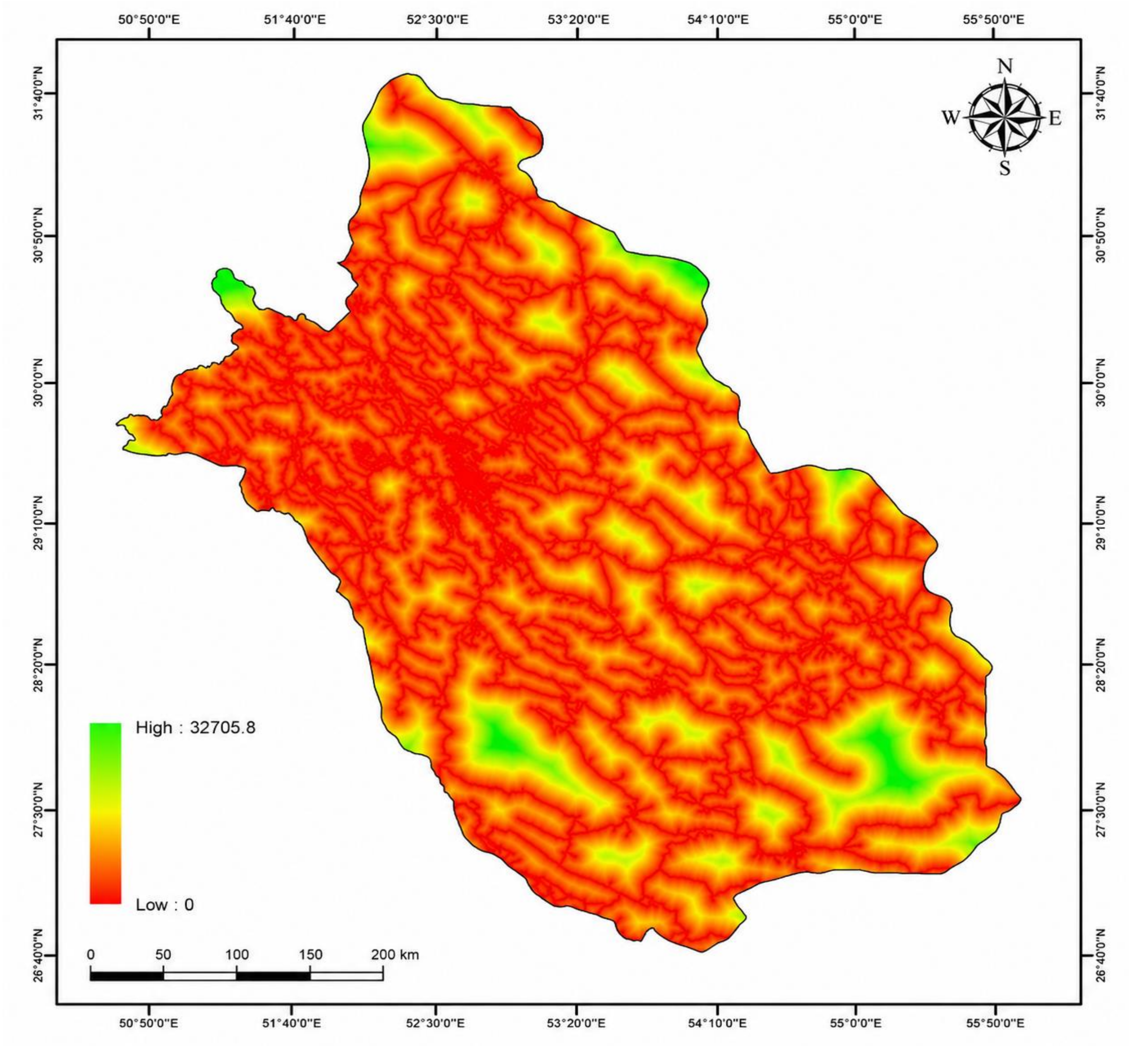

Figure 8. Distance map from the road, the highest distance from road in study area (Fars province) is 32705.8 meters, and the minimum one is 0 meter.

Table 7. Geographical distribution of fire incidents according to distance map from roads

Distance (m)	Fire Incidents No.	Fire Incidents (%)
0-650	585	53.71
650-1700	308	28.28
1700-3000	137	12.58
3000-5100	54	4.95
5100-13459	5	0.45
Total	1089	100.00

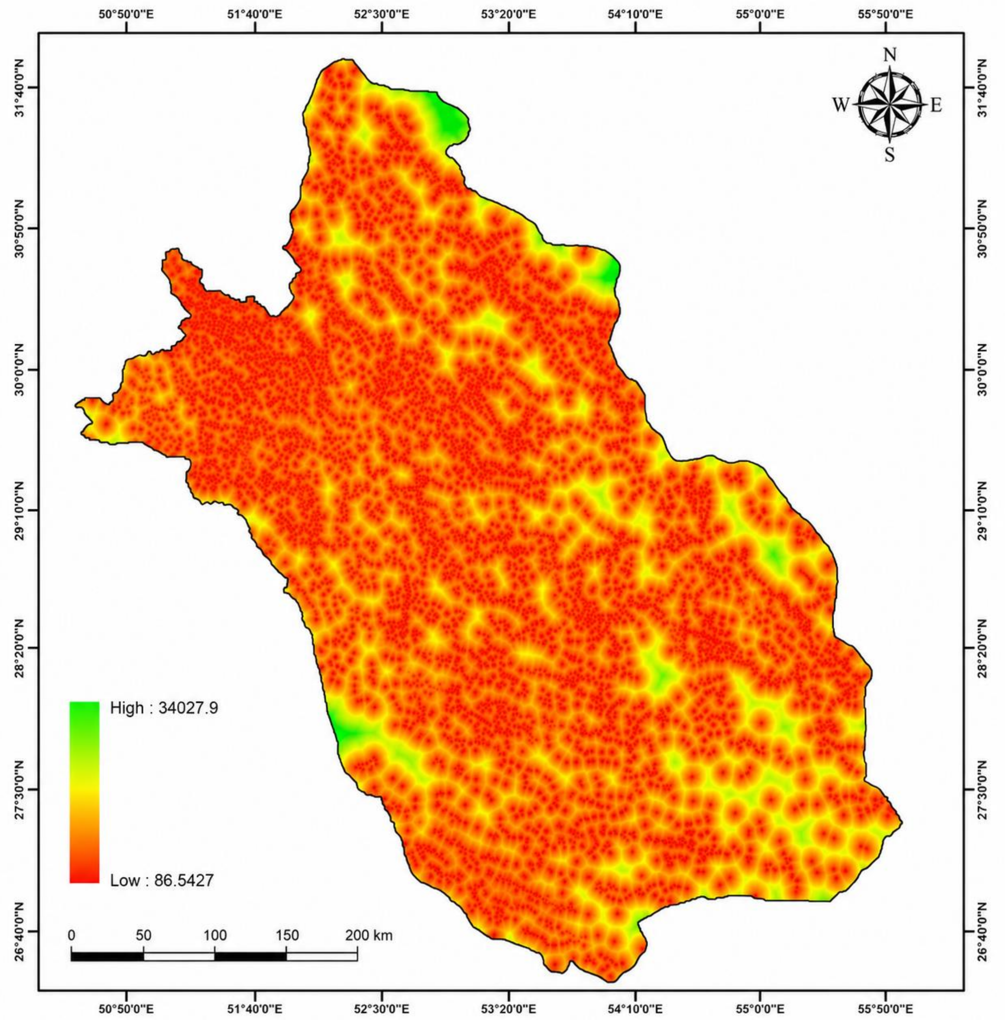

Figure 9. Distance map from the settlement, the highest distance from the settlement in study area (Fars province) is 34027.9 (m), and the minimum one is 86.5427 (m)

Table 8. Geographical distribution of fire incidents according to distance map from the settlement

Distance(m)	Fire Incidents No.	Fire Incidents (%)
0-2300	490	44.99
2300-4900	436	40.03
4900-8400	144	13.22
8400-15900	19	1.74
15900-34227	0	0.00
Total	1089	100.00

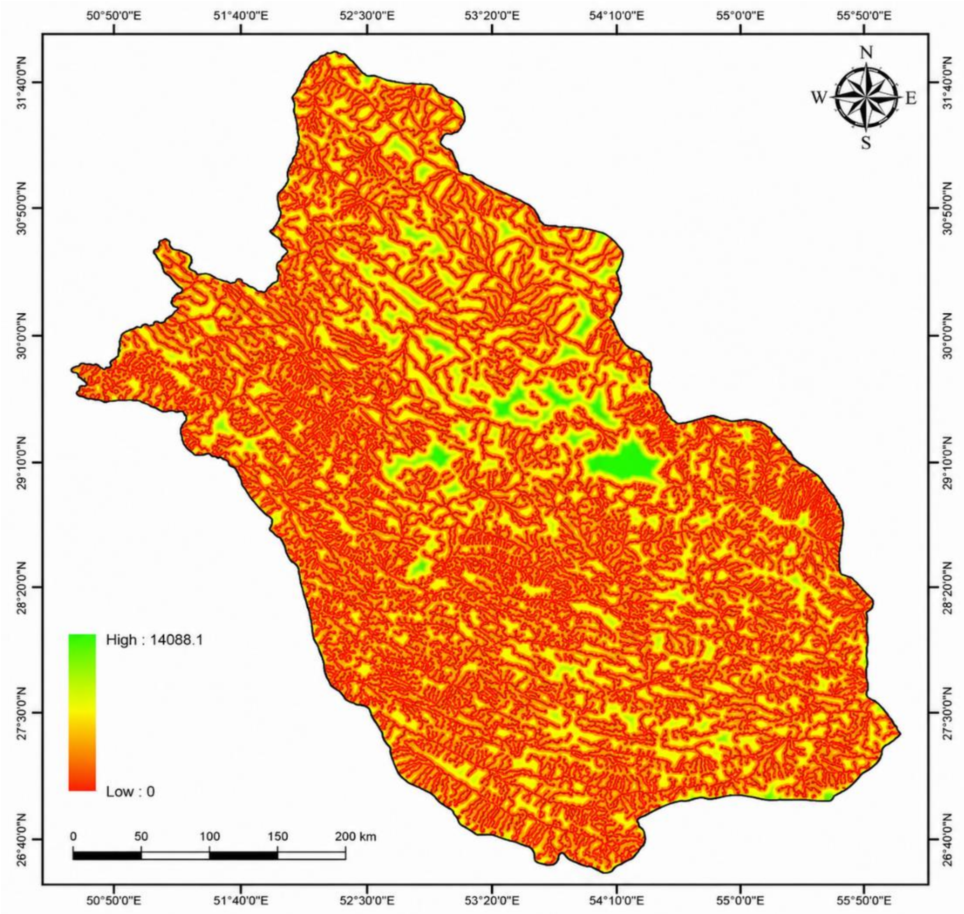

Figure 10. Distance map from the river, the highest distance from the river in Fars province is 14088.1 (m), and the minimum distance is 0 (m)

Table 9. Geographical distribution of fire incidents according to distance map from the river

Distance(m)	Fire Incidents No.	Fire Incidents (%)
0-700	417	38.29
700-1600	391	35.90
1600-2800	203	18.64
2800-5300	75	6.88
5300-12592	3	0.27
Total	1089	100.00

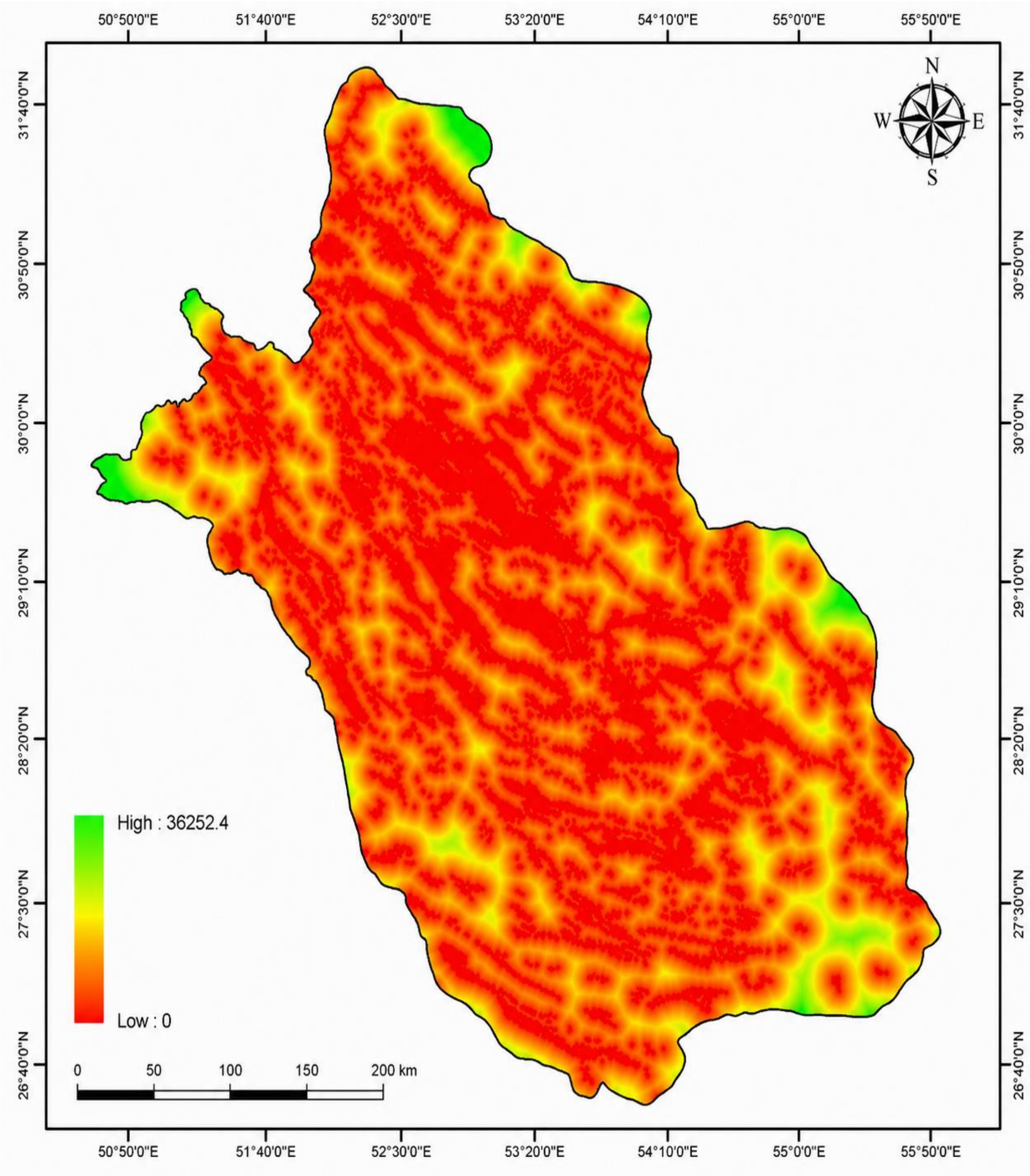

Figure 11. Distance from agricultural land, the highest distance from the agricultural land in Fars province is 36252.4 (m), and the minimum distance is 0 (m)

Table 10. Geographical distribution of fire incidents according to distance map from agricultural land

Distance (m)	Fire Incidents No.	Fire Incidents (%)
0-1600	628	57.66
1600-4000	315	28.92
4000-7300	123	11.29
7300-13000	21	1.92
13000-31045	2	0.18
Total	1089	100.00

Figure 12 shows the land use classification for Fars province by using Sentinel-2 information. There are land use types such as Residential Area, Wetland, Reedbed, Salt Marsh, Shrubland, Bare Land, Agricultural Land, Rangeland, Forest, Clay Land and Water Bodies.

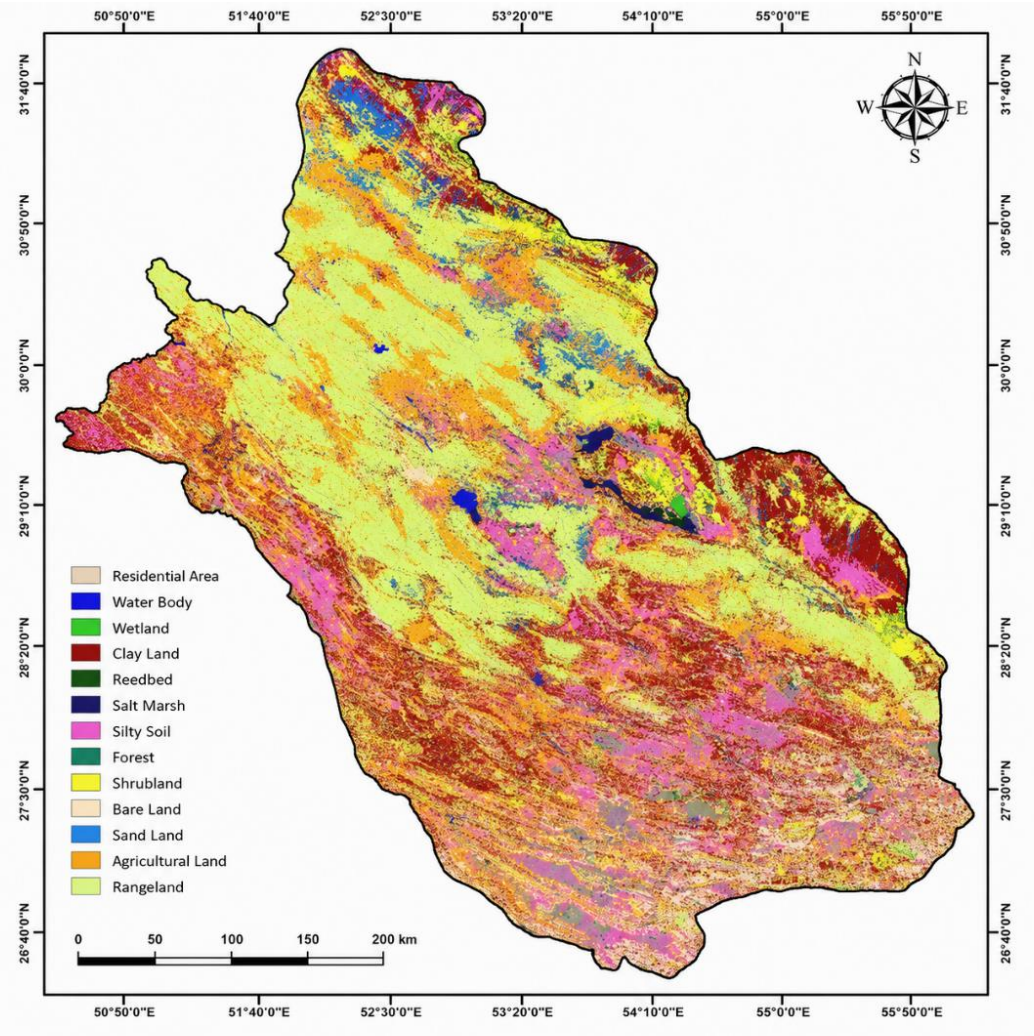

Figure 12. Land use map of Fars province, including Residential Area, Wetland, Reedbed, Salt Marsh, Shrubland, Bare Land, Agricultural Land, Rangeland, Forest, Clay Land and Water Bodies (based on Sentinel-2 product)

3.4. Climatic Variables

For this variable, layers / maps such as Absolute Maximum Summer Temperature, Average Summer Precipitation, and Average Summer Relative Humidity were also prepared (According to Figure 13). Absolute Maximum Summer Temperature in study area represented in section (a), the highest temperature was around 47 ℃ and the lowest one was 35 ℃, during summer. The next section (b) is related to the Average Precipitation (mm) during summer, and the range of values was between 7.73175 and 0.216956. Average Relative Humidity illustrated in section (C), and the highest Humidity was roughly 27.6 % and the lowest one was 22.78%, during summer.

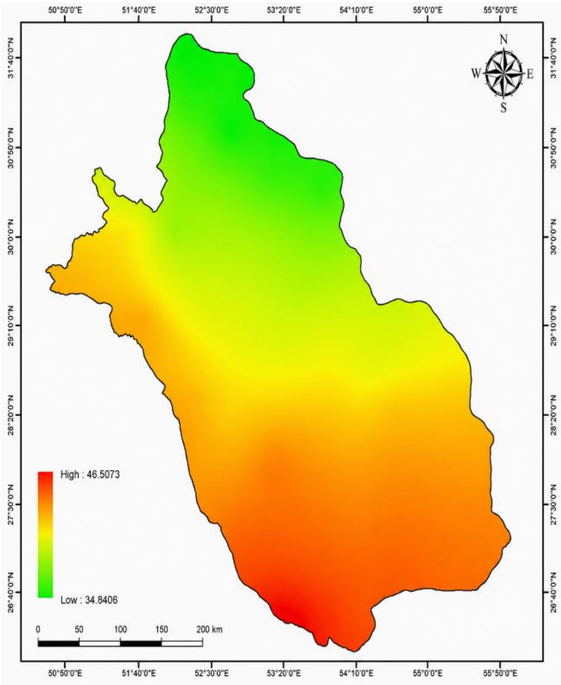

(a): Absolute Maximum Summer Temperature (℃) map

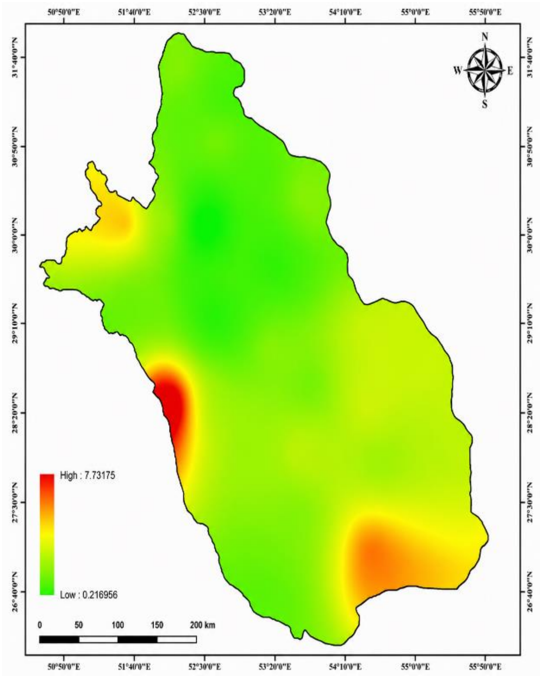

(b): Average Summer Precipitation (mm) map

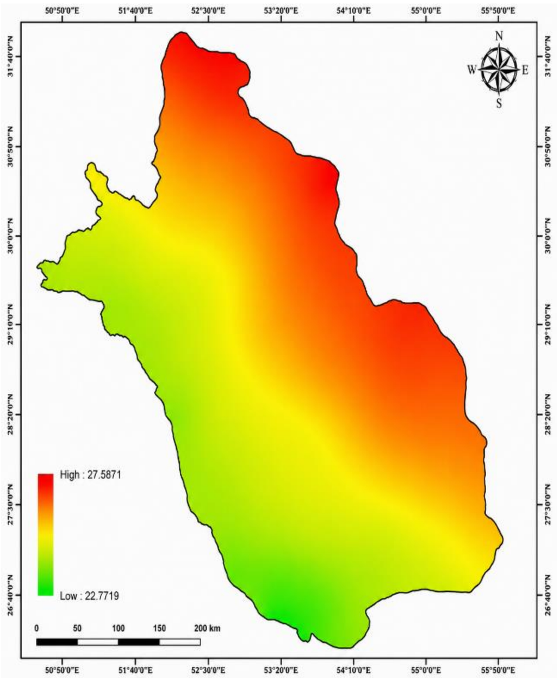

(c): Average Summer Relative Humidity (%) map

Figure 13. Climatic Variables maps including Absolute Maximum Temperature (℃), Average Precipitation (mm), and Average Summer Relative Humidity (%) in Fars province during summer.

3.5. Random Forest Model

For modeling, training data is necessary. For this section training and validation points were prepared and the results are illustrated in Figure14. These points were prepared after reviewing satellite images and matching them with ground measurement data (2178), and then 75 percent (1633) of them were used for training and 25 percent (545) of them were used for validation. In fact, this map is only to show the distribution of the relative positions of training points and validation points. Finally, after preparing the relevant maps and points, the Random Forest modeling process was carried out, and Figure 15 was obtained as a fire risk prediction map in Fars Province as final output.

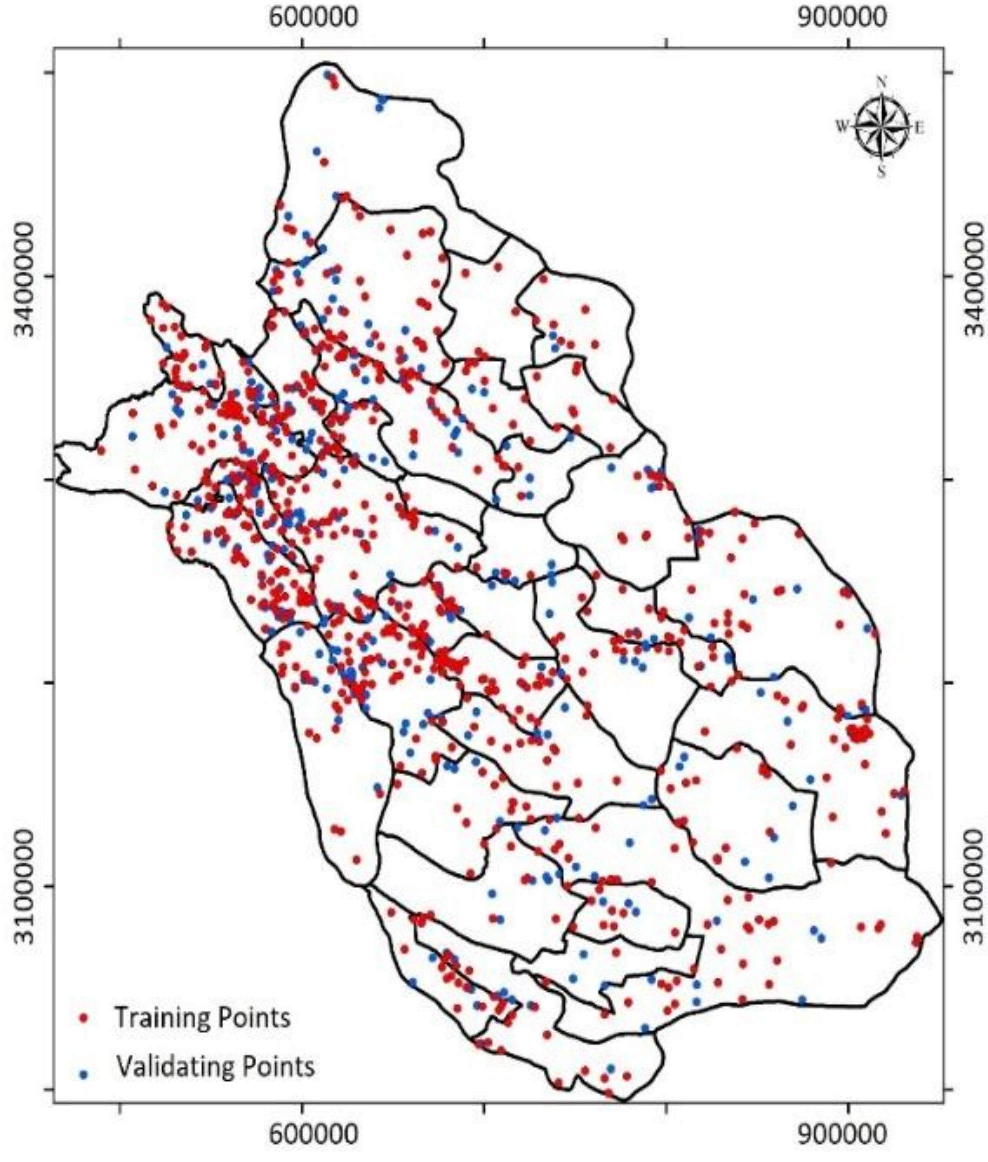

Figure 14. Distribution map of relative location of training and validation points based on RS and ground data. Training points are about fire locations (burned areas) in red and validation points showed in blue.

The final fire risk map is shown in Figure 16. The Random Forest model produces a continuous probability of fire occurrence for each pixel, ranging from 0 (lowest risk) to 1 (highest risk). Then, we classified this continuous output into three risk categories using the Equal Interval method. Based on the probability distribution across Fars Province, the thresholds were set as follows: Low Risk (0–0.33), Moderate Risk (0.33–0.66), and High Risk (0.66–1). According to the map, the western parts of the province fall into the High-Risk class, the southern parts into the Moderate Risk class, and the northern and eastern parts into the Low-Risk class.

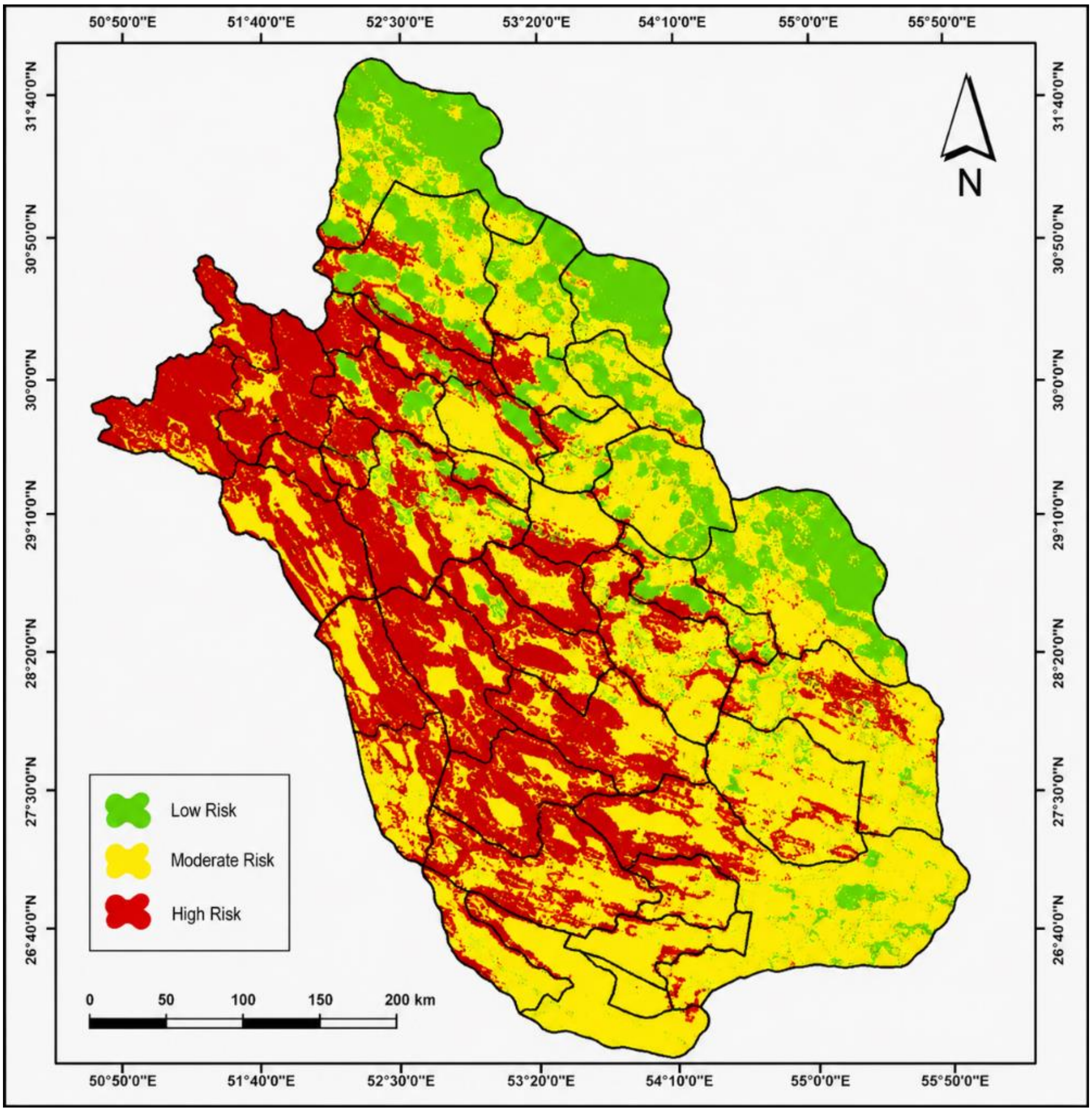

Figure 15. Final Fire risk prediction map including three sections (Low Risk, Moderate Risk, High Risk) in Fars Province

3.6. Assessment

Strong performance in forecasting fire risk was shown by the Random Forest model, which was built using 12 predictive factors from physiographic, meteorological, anthropogenic, and land cover categories. To ensure a comprehensive and robust evaluation, a set of complementary accuracy metrics was employed. As presented in Table 11, the model achieved an AUC of 0.93, a TSS of 0.85, an overall accuracy of 88%, and a Kappa coefficient of 0.83. These values collectively demonstrate excellent discriminatory power and a high level of agreement between predicted and observed fire occurrences. The results confirm the model's reliability and further support the significance of the selected factors in explaining fire susceptibility across Fars Province.

Table 11. Accuracy Assessment of RF model

Metric	Value
AUC	0.93
TSS	0.85
Kappa	0.83
Overall Accuracy	0.88

3.7. Sensitivity Analysis

The importance of independent variables in predicting fire risk across the Fars province was determined based on sensitivity analysis (Figure 16). According to the findings, Land Use (23.6%), Vegetation Type (18.7%), and Absolute Maximum Summer Temperature (14.8%) were identified as the most important variables in this study. On the other hand, Distance from Rivers (0.6%) and Geographical Directions (Aspect) (0.2%) played the least role in this modeling.

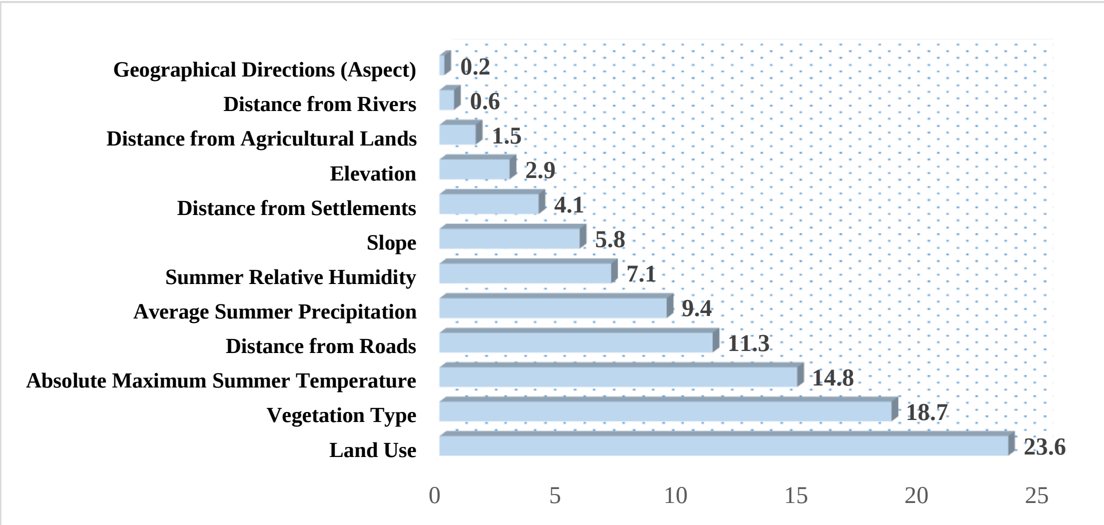

Figure 16. Sensitivity analysis result of RF model (x-axis represented the rate of importance of variables and Y- axis represented the titles of 12 variables). Land use and vegetation type were played the important roles in modeling and distance from Rivers and Aspect were the lowest important variables in modeling.

4. Discussion

Using a collection of twelve anthropogenic and environmental variables, a Random Forest (RF) model was used in this work to create a fire hazard map for Fars Province. The model showed good prediction performance. A significant degree of agreement between the model's predictions and historically recorded fire incidents was demonstrated by the validation based on the kappa coefficient, which produced a value of 83%.

The utilities of the machine learning method, like RF, in this field (risk fire map) have been well demonstrated in various geographical regions. In a case in southeastern Australia, a combination of RF in classification mode and remote data (Sentinel-2) was used to determine fire severity. The results showed an average accuracy of 88% across severity classes, with notably high accuracy (>95%) for unconstrained and extreme severity areas (Gibson *et al*., 2020). The criteria for severity mapping in temperate Australian forests using Landsat and RF were the main focus of the other investigation. According to the findings, it took about 300 training points per class over several fires to get the best accuracy of about 88% for wildfires (Collins *et al*. 2020).

In various fields like susceptibility mapping of fire, RF is frequently compared with other models. In Firouzabad, a municipality in Iran's Fars province, an RF model (accuracy 87.6%, AUC=0.876) outperformed a Bayesian model (80.7%) in mapping fire vulnerability, with elevation and precipitation identified as critical drivers (Noroozi *et al*., 2023). Using integrated approaches such as a combination of RF and Support Vector Machine (SVM) in Serbia, the result illustrated the highest accuracy (AUC=0.848), slightly outperforming the individual models (Gigovi´c *et al*., 2019). In Eastern Serbia, RF (AUC=94.5%) performed marginally better than Logistic Regression (LR, AUC=94.2%) for probability mapping (Milanovi´c *et al*., 2020). A new comparison in Hefei City, China, showed that RF produced (correlation 0.797) more reliable generalized forecasts at the city scale, whereas spatial econometric models combined with RF (a spatial autocorrelation model) offered a superior fit (correlation 0.875) for explaining spatial structure (Song *et al*., 2017). At the regional scale, in Fujian Province, RF (AUC~0.93, accuracy 85.5%) greatly outperformed LR in Fujian Province and determined that temperature, relative humidity, and sunshine hours were the main causes of fire occurrence (Guo *et al*., 2016).

Overall, our findings demonstrate and validate the Random Forest algorithm's resilience and broad applicability for mapping fire intensity and vulnerability in various ecosystems. Moreover, the RF model’s performance was highly accurate, and the key predictive variables were highly context-specific, shaped by localized environments and human factors.

5. Conclusions

This study successfully established a robust and highly accurate wildfire risk prediction model for Fars Province, Iran, by leveraging the powerful integration of the Random Forest (RF) machine learning algorithm with multi-source geospatial data, primarily derived from remote sensing platforms like Sentinel-2 and ALOS PALSAR. The model effectively deciphered the complex, non-linear interactions between twelve critical drivers of fire occurrence, encompassing physiographic, climatic, human activity, and vegetation factors. Variable importance analysis revealed that land use, vegetation type, and absolute maximum summer temperature were the most dominant predictors of fire occurrence in Fars Province, underscoring the significant role of anthropogenic land cover patterns, fuel type distribution, and thermal climatic conditions in driving fire risk. In contrast, physiographic variables such as elevation and aspect, as well as distance from rivers, played a relatively minor role in the model.

The model was rigorously trained and validated on a substantial and verified dataset of 1,089 historical fire incidents, with its performance quantitatively affirmed using multiple metrics, Kappa coefficient (83%), AUC (0.93), TSS (0.85), and overall accuracy (88%). Land Use, Vegetation Type, and Absolute Maximum Summer Temperature variables played important roles in this process. The resultant fire risk map provides a spatially explicit and reliable stratification of the province into distinct zones of susceptibility, from very low to very high risk. This output transcends a mere academic exercise; it serves as a vital decision-support tool for land managers and policymakers in this ecologically diverse and vulnerable region. The practical implications of this research are profound. It enables a strategic paradigm shift from reactive firefighting to proactive, science-based risk management. Authorities can now prioritize areas for targeted mitigation strategies, such as fuel load management through controlled burns, the strategic creation of firebreaks, and public awareness campaigns focused on high-risk communities. Furthermore, it allows for the optimized pre-positioning of firefighting resources during the peak fire season, potentially reducing response times and minimizing damage.

We explicitly acknowledge that the current climatic predictors do not capture conditions driving the remaining 14% of fires that occurred outside summer, and that these events may be under-represented by the model. We note that incorporating season-specific climatic layers (e.g., spring/autumn temperature and precipitation) for these minority cases is a valuable direction for future work.

For future research, integrating dynamic, near-real-time variables such as live fuel moisture content, wind speed, and drought indices could further enhance the model's temporal resolution and predictive accuracy for operational early warning systems. Additionally, applying this scalable and transferable RF-based framework to other ecologically comparable regions in Iran could test its generalizability and pave the way for a standardized, national-level fire risk assessment protocol. Ultimately, this work provides a foundational tool for building more resilient landscapes and safeguarding both natural ecosystems and human communities against the growing threat of wildfires.

Acknowledgment

The authors would like to thank all participants in the present study, especially Mr. Khabazi and Mr. Raouft.

Author Contributions

Conceptualization, S.K.A.; methodology, M.R.K.; software, M.R.K.; validation, M.R.K. and M.T.; formal analysis, M.R.K.; investigation, M.T.; resources, M.T.; data curation, M.T.; writing original draft preparation, E.A.-F.; writing review and editing, E.A.-F. and S.K.A.; visualization, M.R.K.; supervision, S.K.A.; project administration, S.K.A. and M.R.K All authors have read and agreed to the published version of the manuscript.

Ethical considerations

The authors avoided from data fabrication and falsification.

Funding

This research did not receive any specific grant from funding agencies in the public, commercial, or not for-profit sectors.

Competing interests

The authors declare no conflicts of interest.

Data availability

Remote sensing Data is available on official websites.

Conflict of interest

The authors declare no conflict of interest.

References

Ahani, H., Kherad, M., Kousari, M. R., Rezaeian-Zadeh, M., Karampour, M. A., Ejraee, F., & Kamali, S. (2012). An investigation of trends in precipitation volume for the last three decades in different regions of Fars province, Iran. *Theoretical and applied climatology*, 109(3), 361-382. DOI 10.1007/s00704-011-0572-z.

Asadi-Fard, E., Falahatkar, S., Tanha Ziarati, M., Zhang, X. (2024). A new perspective on estimation of gas flaring volume from space: OLI/TIRS, VIIRS, and TROPOMI. *Journal of Geophysical Research: Atmospheres*. 129(11), 1-12. https:// doi.org/ 10.1029/ 2023JD039524.

Azadi, S., & Karimi-Jashni, A. (2016). Verifying the performance of artificial neural network and multiple linear regression in predicting the mean seasonal municipal solid waste generation rate: A case study of Fars province, Iran. *Waste management*, 48, 14-23. http://dx.doi.org/10.1016/j.wasman.2015.09.034.

Belgiu, M., & Drăguţ, L. (2016). Random forest in remote sensing: A review of applications and future directions. *ISPRS journal of photogrammetry and remote sensing*, *114*, 24-31. https://doi.org/10.1016/j.isprsjprs.2016.01.011.

Bar, S., Parida, B. R., & Pandey, A. C. (2020). Landsat-8 and Sentinel-2 based forest fire burn area mapping using machine learning algorithms on GEE cloud platform over Uttarakhand, Western Himalaya. *Remote Sensing Applications: Society and Environment*, 18, 100324. https://doi.org/10.1016/j.rsase.2020.100324

Chowdhury, E. H., & Hassan, Q. K. (2015). Operational perspective of remote sensing-based forest fire danger forecasting systems. *ISPRS Journal of Photogrammetry and Remote Sensing*, *104*, 224-236. http://dx.doi.org/10.1016/j.isprsjprs.2014.03.011.

Collins, L., Griffioen, P., Newell, G., & Mellor, A. (2018). The utility of Random Forests for wildfire severity mapping. *Remote sensing of Environment*, *216*, 374-384. 10.1016/j.rse.2018.07.005.

Collins, L., McCarthy, G., Mellor, A., Newell, G., & Smith, L. (2020). Training data requirements for fire severity mapping using Landsat imagery and random forest. *Remote Sensing of Environment*, 1-14, https://doi.org/10.1016/j.rse.2020.111839.

Gibson, R., Danaher, T., Hehir, W., & Collins, L. (2020). A remote sensing approach to mapping fire severity in south-eastern Australia using sentinel 2 and random forest. *Remote sensing of environment*, *240*, 1-13. https://doi.org/10.1016/j.rse.2018.07.005.

Gigović, L., Pourghasemi, H. R., Drobnjak, S., & Bai, S. (2019). Testing a new ensemble model based on SVM and random forest in forest fire susceptibility assessment and its mapping in Serbia's Tara National Park. *Forests*, 10(5), 1-21. doi:10.3390/f10050408.

Guo, F., Wang, G., Su, Z., Liang, H., Wang, W., Lin, F., & Liu, A. (2016). What drives forest fire in Fujian, China? Evidence from logistic regression and Random Forests. *International Journal of Wildland Fire*, *25*(5), 505-519. http://dx.doi.org/10.1071/WF15121.

Helman, D. (2018). Land surface phenology: what do we really ‘see’ from space?. *Science of The Total Environment*. 618, 665–673. https://doi.org/10.1016/j.scitotenv.2017.07.237.

Hultquist, C., Chen, G., & Zhao, K. (2014). A comparison of Gaussian process regression, random forests and support vector regression for burn severity assessment in diseased forests. *Remote sensing letters*, *5*(8), 723-732. https://doi.org/ 10.1080/ 2150704X. 2014. 963733.

Forsberg, N.T., Longo, B.M., Baxter, K., & Boutté, M. (2012). Wildfire smoke exposure: A guide for the nurse practitioner. *The Journal for Nurse Practitioners*, 8(2), 98–106. https://doi.org/10.1016/j.nurpra.2011.07.001.

Khabazi, F., Kargar, M., Keshavarz, M. E., Asadi-Fard, E., Salehi, S. and Bayat Shahparast, A. (2025). Site selection of Optimal Areas for Establishing livestock markets Centers by Nomadic Tribes in Fars Province. *Geography and Human Relationships*, 8(2), 530-545. Doi: 10.22034/ gahr.2025 .510862.2418.

Kim, B., Sarkar, S. (2017). Impact of wildfires on some greenhouse gases over continental USA: a study based on satellite data. *Remote Sens. Environ.*, 188, 118–126. https//: doi.org/10.1016/j.rse.2016.10.047.

Ma, W., Feng, Z., Cheng, Z., Chen, S., & Wang, F. (2020). Identifying forest fire driving factors and related impacts in China using random forest algorithm. *Forests*, 11(5), 1-26. doi:10.3390/f11050507.

Meng, R., Wu, J., Schwager, K. L., Zhao, F., Dennison, P. E., Cook, B. D., Brewster, K., Green, T.M. & Serbin, S. P. (2017). Using high spatial resolution satellite imagery to map forest burn severity across spatial scales in a Pine Barrens ecosystem. *Remote Sensing of Environment*, *191*, 95-109. 10.1016/j.rse.2017.01.016.

Michael, Y., Helman, D., Glickman, O., Gabay, D., Brenner, S., & Lensky, I. M. (2021). Forecasting fire risk with machine learning and dynamic information derived from satellite vegetation index time-series. *Science of The Total Environment*, *764*, 1-10. https://doi.org/10.1016/j.scitotenv.2020.142844.

Milanović, S., Marković, N., Pamučar, D., Gigović, L., Kostić, P., & Milanović, S. D. (2020). Forest fire probability mapping in eastern Serbia: Logistic regression versus random forest method. *Forests*, *12*(5), 1-17. https://dx.doi.org/10.3390/f12010005.

Meddens, A. J., Kolden, C. A., & Lutz, J. A. (2016). Detecting unburned areas within wildfire perimeters using Landsat and ancillary data across the northwestern United States. *Remote Sensing of Environment*, *186*, 275-285. 10.1016/j.rse.2016.08.023.

Noroozi, F., Ghanbarian, G., Safaeian, R., & Pourghasemi, H. R. (2024). Forest fire mapping: a comparison between GIS-based random forest and Bayesian models. *Natural Hazards*, 120(7), 6569-6592. https://doi.org/10.21203/rs.3.rs-3476357/v1.

Oliveira, S., Oehler, F., San-Miguel-Ayanz, J., Camia, A., & Pereira, J.M.C. (2012) Modeling spatial patterns of fire occurrence in Mediterranean Europe using Multiple Regression and Random Forest. *Forest Ecology and Management*, 275, 117–129. http://dx.doi.org/10.1016/j.foreco.2012.03.003.

Parks, S. A., Holsinger, L. M., Koontz, M. J., Collins, L., Whitman, E., Parisien, M. A., Loehman, R.A., Barnes, J.L., Bourdon, J.-F., Boucher, J., Boucher, Y., Caprio, A.C., Collingwood, A., Hall, R.J., Park, J., Saperstein, L.B., Smetanka, C., Smith, R.J., & Soverel, N. (2019). Giving ecological meaning to satellite-derived fire severity metrics across North American forests. Remote Sensing, 11(14), 1735.

Polat, S., Ghasemi Aghbash, F., & Mahdavi, A. (2020). Forest fire hazard zone mapping in Ilam county forests. *Forest Research and Development*, 6(1), 135-152. doi: 10.30466/jfrd.2020.120830.

Silva, I. T., Pessi, D. D., Silva, N. M., Silva, C. L. O. C., Guaraldo, E., & Paranhos Filho, A. C. (2021). Técnicas de processamento de imagens para treinamento de fotointerpretes na avaliação visual de áreas úmidas e de manchas e cicatrizes de queimadas ou incendios. *Revista de Geociências do Nordeste*, 7(2), 57-67. DOI: 10.21680/2447-3359.2021v7n2ID23310

Song, C., Kwan, M. P., Song, W., & Zhu, J. (2017). A comparison between spatial econometric models and random forest for modeling fire occurrence. *Sustainability*, 9(5), 1-21. doi:10.3390/su9050819.

Szpakowski, D.M., Jensen, J.L.R. (2019). A review of the applications of remote sensing in fire ecology. *Remote Sensing*, 11, 2638. https://doi.org/10.3390/rs11222638.

Yang, S., Lupascu, M., & Meel, K. S. (2021). Predicting forest fire using remote sensing data and machine learning: The Thirty-Fifth AAAI Conference on Artificial Intelligence (AAAI-21) (pp. 14983-14990). DOI: https://doi.org/10.1609/aaai.v35i17.17758.

Yousefi Kebriya, A.R., Nadi, M., & Yousefi Kebriya, H. (2025). Analysis of the Impact of Agricultural Fires on Air Quality in Mazandaran Province Using Satellite Data. *Journal of the Climate Change research*, 6 (22), 25-44. DOI: 10.30488/CCR.2025.492951.1260.

Yu, B., Chen, F., Li, B., Wang, L., & Wu, M. (2017). Fire risk prediction using remote sensed products: A case of Cambodia. *Photogrammetric Engineering & Remote Sensing*, *83*(1), 19-25. doi: 10.14358/PERS.83.1.19.